Downloaded via DTIC NATL TECH INFORMATION CTR on April 3, 2020 at 13:43:45 (UTC).
See https://pubs.acs.org/sharingguidelines for options on how to legitimately share published articles.

ARTICLE

HfO_2 on MoS_2 by Atomic Layer Deposition: Adsorption Mechanisms and Thickness Scalability

Stephen McDonnell,* Barry Brennan, Angelica Azcatl, Ning Lu, Hong Dong, Creighton Buie, Jiyoung Kim, Christopher L. Hinkle, Moon J. Kim, and Robert M. Wallace*

Department of Materials Science and Engineering, University of Texas at Dallas, Richardson, Texas 75080, United States

ABSTRACT We report our investigation of the atomic layer deposition (ALD) of HfO_2 on the MoS_2 surface. In contrast to previous reports of conformal growth on MoS_2 flakes, we find that ALD on MoS_2 bulk material is not uniform. No covalent bonding between the HfO_2 and MoS_2 is detected. We highlight that individual precursors do not permanently adsorb on the clean MoS_2 surface but that organic and solvent residues can dramatically change ALD nucleation behavior. We then posit that prior reports of conformal ALD deposition on MoS_2 flakes that had been exposed to such organics and solvents likely rely on contamination-mediated nucleation. These results highlight that surface functionalization will be required before controllable and low defect density high-κ/MoS_2 interfaces will be realized. The band structure of the HfO_2/MoS_2 system is experimentally derived with valence and conduction band offsets found to be 2.67 and 2.09 eV, respectively.

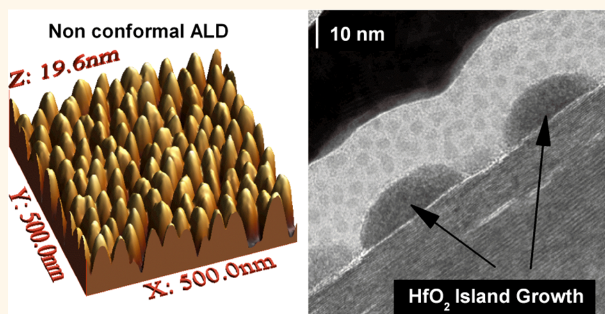

KEYWORDS: HfO_2 · MoS_2 · TMD · high-κ · ALD · band offsets · nanoelectronics

Since the successful exfoliation of graphene and the demonstration of the remarkable electronic properties of that material,[1] considerable research has been carried out on both large-area synthesis of graphene[2,3] and its potential device applications.[4,5] One of the primary limitations in implementing graphene as a transistor channel material is the difficulty in opening a band gap, which is required for many device applications.[6−8] The transition metal dichalcogenide (TMD) family of materials are 2-D crystals, similar to graphite, that can be exfoliated to obtain stable, single monolayers. Unlike graphite/graphene, TMDs can exhibit metal or semiconducting properties through the proper selection of transition metal or chalcogen in the crystal, and their band gaps can be tunable with thickness, making them suitable for a wide range of electronic and optoelectronic device applications.[9] Relative to graphene, the initial reports of carrier mobilities for exfoliated single-layer MoS_2 on SiO_2 were low (0.1−10 cm^2/Vs).[6,10] However, Jena *et al.*[11] predicted that the enhanced Coulombic impurity scattering present in free-standing 2-D materials can be reduced by coating them with high-κ dielectrics. An improved mobility has also been experimentally observed[6,12] by the deposition of a high-κ dielectric on top of a 2-D channel which is already screened on the backside by an insulating substrate. As such, these materials offer greater flexibility with respect to graphene for integration into currently established device architectures.

Recent publications demonstrating transistor devices with MoS_2[6,7,13] and WSe_2[14] channels utilized atomic layer deposition (ALD) to grow high-κ dielectrics, using H_2O as the oxidizing precursor, with no intentional predeposition surface functionalization reported, such as those employed for graphene, for example, NO_2,[15] metal seed layers,[16] organic seed layers,[17] or ozone (O_3).[15,18] The adsorption mechanism of TMA/H_2O on MoS_2 and hexagonal boron nitride (hBN) was studied in more detail by Liu *et al.*,[19] and the proposed physisorption mechanism suggests that the deposition behaves similarly to that observed for TMA/NO_2 on

* Address correspondence to stephenmcd@utdallas.edu, rmwallace@utdallas.edu.

Received for review September 11, 2013 and accepted October 13, 2013.

Published online October 14, 2013
10.1021/nn404775u

© 2013 American Chemical Society

carbon nanotubes[15] and TMA/O_3 with graphene.[18] In the case of TMA/O_3 ALD on graphite/graphene, ALD growth was dominated by reactions with residual surface contamination rather than reactions with the basal plane,[20,21] and similar phenomenon may also play a role on the MoS_2 surface. However, the fact that uniform ALD on MoS_2 has been reported, apparently without intentional surface functionalization or seeding layers, at temperatures up to 200 °C has led to the suggestion that nucleation in ALD may be considerably different on TMDs than on graphite.[19]

In this article, we report on the physical, electrical, and chemical properties of the HfO_2/MoS_2 interface and discuss the initial nucleation of ALD on this surface using *in situ* methods. Large-area (~5 × 5 mm) MoS_2 crystals are used as substrates for the dual purpose of allowing chemical analysis with X-ray photoelectron spectroscopy (XPS) and also for simulating large-area substrates that have not been exposed to organics, solvents, and adhesives that are commonly used to transfer flakes. It is shown that growth of HfO_2 using tetrakis(dimethylamino)hafnium (TDMA-Hf) and H_2O precursors without intentional functionalization layers is not a scalable process. This is demonstrated by showing that parts of the MoS_2 surface are still exposed after 150 ALD cycles of HfO_2 (nominally corresponding to ~15 nm) have been deposited, with 15−17 nm islands being observed by atomic force microscopy (AFM) and transmission electron microscopy (TEM). Samples that have been deliberately and controllably contaminated with organics and/or solvents are shown to result in markedly different HfO_2 topography. The initial adsorption of the ALD precursors is monitored with *in situ* XPS, and a potential mechanism for deposition is discussed. By combining XPS and photoconductivity measurements, an experimental measurement of the band offsets in this system is provided.

RESULTS AND DISCUSSION

The previous reports of high-κ dielectrics deposited by ALD on both MoS_2 and WSe_2 surfaces, discussed above, have been limited to relatively thick (≥10 nm) oxide layers. Radisavljevic *et al.*[6] deposited 30 nm of HfO_2 on single-layer MoS_2, and Wang *et al.*[13] used a similar process to deposit 20 nm on bilayer MoS_2. Fang *et al.*[14] deposited 17 nm of ZrO_2 on WSe_2, and Liu *et al.*[7,19] have deposited 10 nm of Al_2O_3 on MoS_2 and hBN.

For TMDs to be useful as channel materials in top-gated devices, the growth of conformal ultrathin high-κ dielectrics will be required. Shown in Figure 1 is an investigation of the scalability of HfO_2 ALD on exfoliated bulk MoS_2 using TDMA-Hf and H_2O at 200 °C. The deposition parameters were kept similar to those previously reported,[6] which included using a {TDMA-Hf/N_2 purge/H_2O/N_2 purge/H_2O/N_2 purge} cycle. Further details of this process are included in the Supporting Information. The deposition rate reported

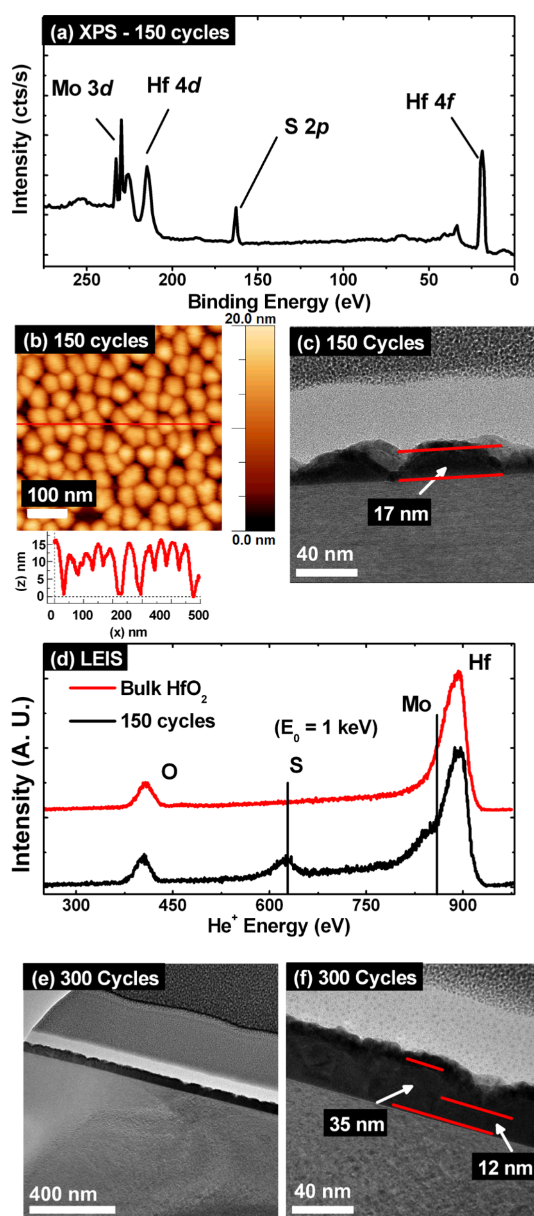

Figure 1. (a) XPS for HfO_2/MoS_2 stack after 150 cycles of ALD; (b) 0.5 × 0.5 μm AFM image of the same HfO_2/MoS_2 stack; (c) TEM images of a $Pt/SiO_2/Pd/HfO_2/MoS_2$ stack with 150 cycles of HfO_2 ALD on MoS_2 (40 nm scale bar). (d) LEIS spectra taken after 150 cycles (black, bottom) and bulk HfO_2 on Si (red, top). (e) TEM image of a $Pt/SiO_2/Pd/HfO_2/MoS_2$ stack with 300 cycles of HfO_2 ALD on MoS_2 (400 nm scale bar). (f) TEM image of a $Pt/SiO_2/Pd/HfO_2/MoS_2$ stack with 300 cycles of HfO_2 ALD on MoS_2 (40 nm scale bar).

for this process on MoS_2 was 0.19 nm/cycle,[6] which is double the value of 0.09 nm/cycle that is normally reported for TDMA-Hf/H_2O on more reactive SiO_2 and III−V substrates.[22,23] Using the electron attenuation lengths for electrons from the Mo 3d and S 2p core-levels in HfO_2, it can be shown that a conformal layer of >5 nm will reduce the intensity of the Mo 3d and S 2p core-level features to less than 1% of their original values.[24]

In contrast, the XPS shown in Figure 1a shows that even 150 cycles of HfO_2 ALD (~15 nm) is insufficient to

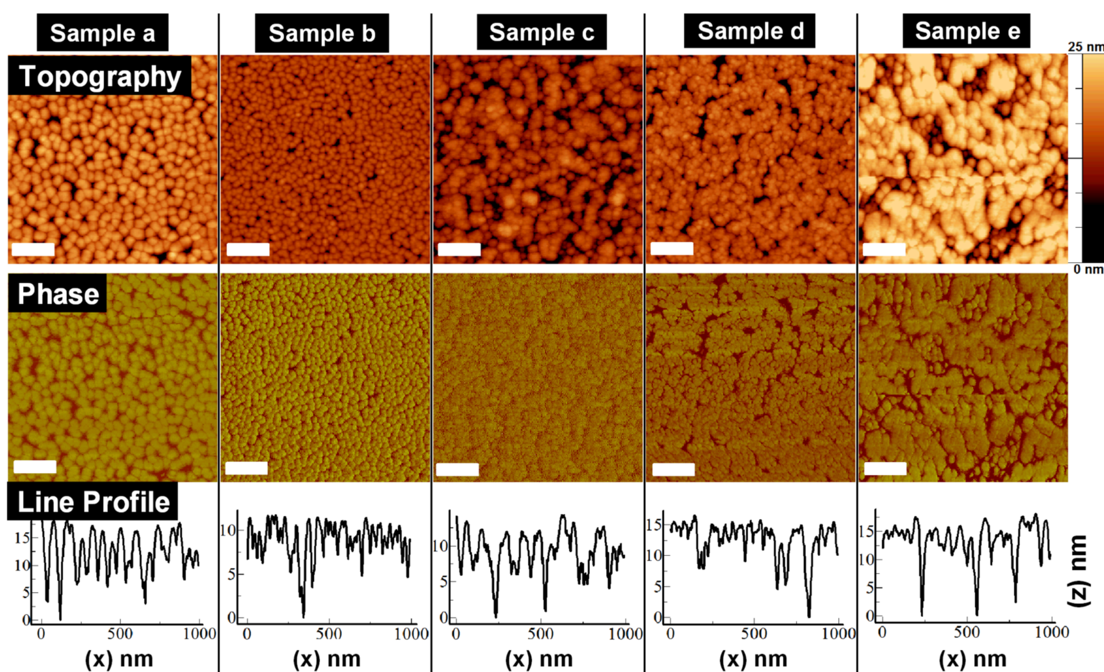

Figure 2. Atomic force microscopy topography, phase images, and line profiles for (a) MoS_2 cleaned by mechanical exfoliation; (b) MoS_2 cleaned by mechanical exfoliation and submerged in acetone for 2.5 h; (c) MoS_2 cleaned by mechanical exfoliation and submerged in NMP for 2.5 h; (d) MoS_2 cleaned by mechanical exfoliation, coated with PMMA, and submerged in acetone for 2.5 h; (e) MoS_2 cleaned by mechanical exfoliation, coated with PMMA, and submerged in NMP for 2.5 h. The $x-y$ scale bars are 200 nm; z-axis is 0−25 nm; phase z-axis is −10 to +10°.

reduce the Mo 3d and S 2p signals to below detection limits. The AFM image shown in Figure 1b shows that ALD of 150 cycles of HfO_2 on MoS_2 results in the deposition of islands (height ~15 nm, width ~60 nm), and the high-resolution transmission electron microscopy (TEM) shown in Figure 1c confirms the island growth. *In situ* low-energy ion scattering (LEIS) was employed to further confirm that the HfO_2 does not cover the MoS_2 substrate after 150 cycles of ALD since the detection of S and Mo signals shown by LEIS in Figure 1d is not possible unless these atoms reside on the surface.[25] Figure 1e shows that full coverage of the MoS_2 is possible with more ALD cycles; however, the films are still highly non-uniform with variations of more than 20 nm observed in Figure 1f. This thickness variation was not observed in the previous study by Radisavljevic *et al.*, where the uniform deposition of 30 nm of HfO_2 on MoS_2 was reported.[6] The HfO_2 thicknesses observed in the TEM images suggest a deposition rate of ~0.11 nm/cycle, which is consistent with the ~0.1 nm/cycle estimate from the height of the islands observed by AFM. The observed growth rate is close to the 0.093 nm/cycle that is expected for TDMA-Hf/H_2O ALD on SiO_2 substrates;[22] however, the uniform deposition of HfO_2 directly onto MoS_2 is clearly not observed.

This result is in contrast with the recent reports of conformal ALD on MoS_2 by both Radisavljevic *et al.*[6] and Liu *et al.*[19] that was assumed, by Fang *et al.*,[14] to be replicated on WSe_2. While none of these studies reported the use of an intentional functionalization layer, it should be noted that all reported the transferring of TMD flakes to insulating substrates as well as the subsequent device fabrication.[6,13,14,19] Tape residues were typically "removed" by cleaning with acetone[26] or high-temperature annealing,[27] while device fabrication utilizing e-beam lithography typically involves coating the surface with poly(methyl methacrylate) (PMMA) or other organics followed by removal with solvents.[6,14,27] Transfer-induced residual contamination has been shown previously to be very difficult to completely remove from graphene surfaces, even after UHV annealing.[28,29] Therefore, it is possible that such residues may have played a role in the ALD nucleation.

To test this hypothesis in a controlled manner, 150 ALD cycles of HfO_2 were carried out simultaneously on five MoS_2 samples. Four MoS_2 samples had been deliberately exposed to organic and/or solvent contaminants to simulate the possible residues that would result for exfoliated flake transfers and device fabrication. Since such device fabrication is typically achieved through e-beam lithography using PMMA, this organic was chosen as a sample organic contaminant. The solvents acetone and *N*-methyl-2-pyrrolidone (NMP) were used for this study because rinses or soaks in acetone are commonly reported for tape residue and PMMA removal while NMP provided a second solvent for comparison. The results of this study are shown in Figure 2. A sample that was cleaned by mechanical exfoliation only (Figure 2a) is assumed to be nominally residue-free and served as a control sample for this study. The effect of solvent residues

on ALD nucleation was tested by mechanically exfoliating two separate samples and then immersing them in baths of acetone (Figure 2b) or NMP (Figure 2c) for 2.5 h. The effect of organic residues on ALD nucleation was tested by mechanically exfoliating two separate samples and then spin-coating them with PMMA followed by a PMMA removal step by immersing the sample for 2.5 h in acetone (Figure 2d) or NMP (Figure 2e).

The image in Figure 2a shows the deposition of ~15 nm islands similar to Figure 1b. The deposition of HfO_2 on MoS_2 with acetone residue (Figure 2b) appears qualitatively similar to that of the clean MoS_2; however, all three of the other processes resulted in markedly different film topography, suggesting that organic residue and even a solvent such as NMP can alter subsequent ALD nucleation. The phase images provide extra information because they are sensitive to variations in material properties and suggest that while the NMP-soaked sample still shows large thickness variations, the coverage of the HfO_2 on the MoS_2 substrate, with respect to exfoliated only substrate, is noticeably improved.

This result strongly suggests that the TMD surfaces in the recent reports of FET devices with TDMA/H_2O ALD gate dielectrics on both MoS_2[6,13] and WSe_2[14] as well as in the ALD studies of TMA/H_2O on BN and MoS_2 flakes were unintentionally functionalized.[19] As such, these reports do not reflect the intrinsic susceptibility of TMDs to conformal ALD. Since recent advances in TMD synthesis[30,31] suggest that large-area growth should be possible directly on insulating substrates, it is unlikely that industrial scale TMD-based nanoelectronic device fabrication will involve a mechanical scotch-tape transfer process. Moreover, this lack of nucleation on nonfunctionalized MoS_2 will be a real issue that needs to be addressed.

Since the deposition of HfO_2 on MoS_2 is seen to be nonconformal, a detailed study of the initial precursor adsorption and reactions is required. The initial stages of HfO_2 deposition on exfoliated bulk MoS_2 ("Sample 1"), monitored by half-cycle ALD and *in situ* XPS, are shown in Figure 3. It is clear from the Hf 4f region that no hafnium species are detected after four half-cycle (equivalent to two full cycle) exposures. Similarly, the O 1s region shows that any oxygen is at the limit of detection. In a separate experiment, a freshly exfoliated MoS_2 substrate ("Sample 2") was exposed to two full cycles of ALD after which clear hafnium and oxygen signals are observed. The only differences between these two ALD processes are the time between the precursor pulses and the necessary exposure of the first sample to UHV conditions during each XPS analysis step.

The detection of HfO_2 after two full, *uninterrupted*, cycles of ALD proves that the lack of deposition in the half-cycle experiment cannot be due to insufficient

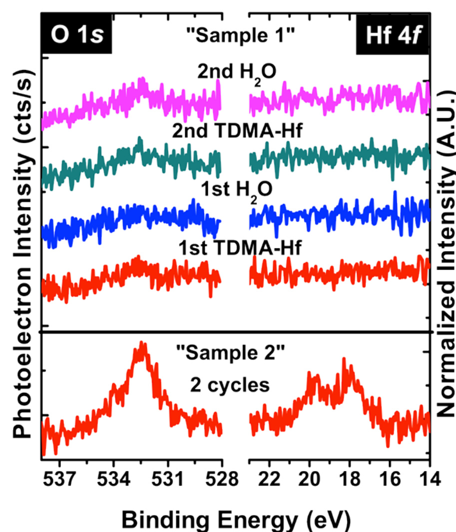

Figure 3. XPS core-level spectra of the O 1s and Hf 4f regions, where the Hf 4f region is referenced to the initial "as-received" spectra to remove the S 3s feature (see Supporting Information for the original data). The spectra are as follows: MoS_2 "Sample 1" after each of four half-cycle HfO_2 ALD exposures separated by >6 h in UHV for XPS analysis, and MoS_2 "Sample 2" after two full HfO_2 ALD cycles with purges times of 5 and 10 s after the TDMA-Hf and H_2O precursor pulses, respectively.

incubation or pulse times. Instead, the deposition process appears to be dependent on the length of time between the precursor pulses. This purge time dependence is consistent with ALD on other inert surfaces such as TMA/NO_2 on carbon nanotubes[15] and TMA/O_3 on annealed graphite[21] and strongly suggests that the deposition of HfO_2 on nonfunctionalized MoS_2 is a process that is achieved by precursor (A) reacting with precursor (B) *on* the MoS_2 surface without either having reacted *with* the MoS_2 surface. Mobile precursors can diffuse for a limited time on the surface before either finding a reaction site or desorbing.[32] Assuming that a precursor can remain mobile on, or in the vicinity of, the surface for durations of 5−10 s, during a N_2 purge in the millibar regime,[19,22] one can envisage that precursor A may be present and still mobile on the sample surface during the pulse of precursor B. Such a situation would allow for reactions between the precursors without either precursor reacting with the MoS_2 surface. The plausibility of this scenario will now be discussed.

The *ideal* ALD process is one where all gaseous and physisorbed precursors are completely removed from the chamber and surface, respectively, during a purge sequence. In practice, this is rarely the case, and there is a nonzero probability of some precursors remaining mobile on the surface throughout such a N_2 purge. For example, Hausmann *et al.*[22] reported that purge times required to fully remove precursors from an ALD reactor are dependent on temperature and can exceed 100 s even at 150 °C and 0.33 mbar of N_2. Also, density functional theory calculations by Liu *et al.*[19] suggested

that, without chemisorption, strong interactions can still occur between precursors and inert surfaces such as MoS_2 and hBN. These interactions would lengthen the lifetime of a precursor on the surface during a N_2 purge. In that study, the supporting experimental evidence was a reduction in deposition rate with increasing temperature while the purge times remained constant at 6 s. Our studies show that at least for TDMA-Hf and H_2O precursors, while the weakly adsorbed precursors appear to remain on the surface throughout N_2 purges for at least 5–10 s, the precursors do not remain on the surface for extended periods of time (*i.e.*, hours). Since HfO_2 is only detected after *consecutive* ALD cycles with short purge times, the reaction product must be more stable on the surface than the individual precursor.

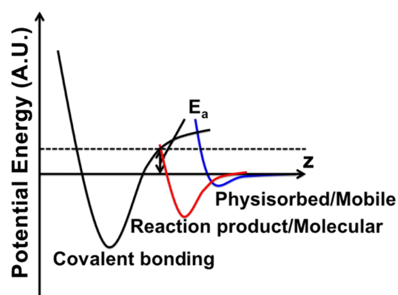

Figure 4. Lennard-Jones-type potential curves illustrating the likely adsorption mechanism based on the purge time-dependent nucleation observed in Figure 3. Without reacting with the MoS_2 surface, physisorbed and mobile precursors desorb from the surface unless they encounter a different precursor. The resultant reaction products are more stable on the surface.

A possible reaction mechanism is illustrated with the aid of Lennard-Jones style potential curves shown in Figure 4. The absence of any observable precursor species in the half-cycle experiments, as shown in Figure 3, suggests a high activation barrier for dissociative adsorption of precursors on the surface (intersection of blue and black curves in Figure 4) and a high probability for the desorption of individual

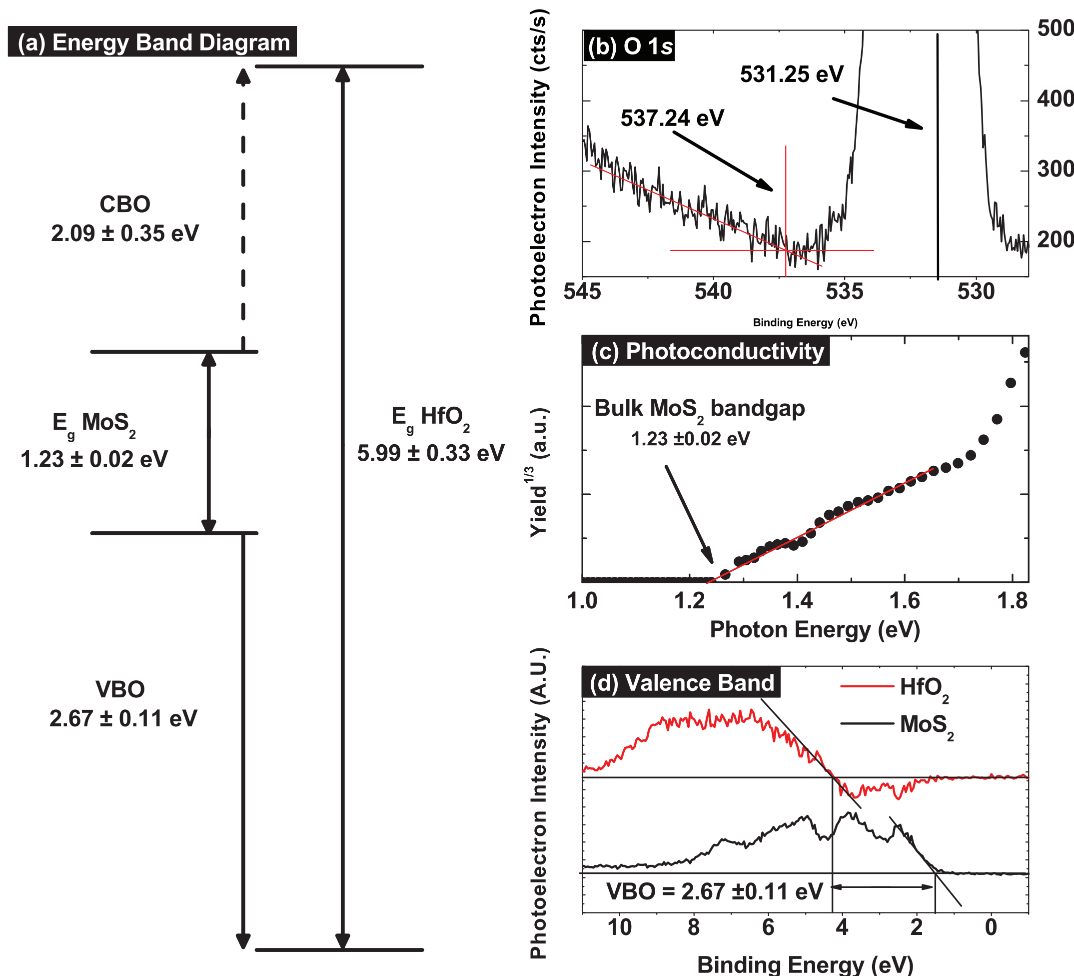

Figure 5. (a) Energy band diagram for HfO_2/MoS_2 stack constructed from experimentally determined band gaps for HfO_2 and MoS_2, and the VBO [solid arrows indicate the experimentally determined values] (b) XPS O 1s core-level spectra showing the onset of the O loss features as well as the position of O–Hf feature, (c) photoconductivity measurement showing an onset in photoyield at 1.23 eV corresponding to the indirect band gap of bulk MoS_2 (the slope change at ~1.7 eV attributed to the additional photoyield[50] of the *direct* band gap of bulk MoS_2), (d) XPS valence band spectra from MoS_2 (black, bottom) and HfO_2/MoS_2 (red, top) energy referenced to S 2p position. The errors quoted in this figure are discussed in the Supporting Information.

precursors. This is most likely due to the low number of reactive sites on the MoS_2 surface. Using short purge times, deposition is observed, suggesting that if both weakly adsorbed metal and oxidant precursors are present on the surface at the same time then a new molecule can be formed, which is more strongly adsorbed to the surface. The lack of observable covalent bonding between the HfO_2 and MoS_2 suggests that the activation energy (E_a) for a dissociative reaction is still high and the HfO_2 remains in a molecular state. Further details of the considered reaction mechanisms are discussed in the Supporting Information.

With a better understanding of how HfO_2 ALD on MoS_2 proceeds on clean MoS_2, in contrast to spuriously functionalized flakes, we can further characterize the HfO_2/MoS_2 system by experimentally determining the band structure at this interface. Designing and understanding devices based on TMDs will require accurate knowledge of the band offsets. Much of the current knowledge of metal oxide/MoS_2 band offsets comes from diagrams constructed based on *reported* electron affinities and work functions for these materials such as for the Ti/MoS_2/Al_2O_3/Si system[33] or for the HfO_2/MoS_2 (single-layer) system.[34] Other works have calculated the band offsets[35] using density functional theory for the HfO_2 in contact with single-layer MoS_2 or combined DFT and photoluminescence to discuss the strain-induced MoS_2 band gap changes[36,37] related to the ALD of metal oxides. It should be noted that the impact of many-electron effects in TMDs remains a topic of intense study for first principle models.[38,39] Since it is now known that the initial reports[6] of high mobilities for single-layer MoS_2 were overestimated,[40,41] it is likely that many future device applications will be based on few- or many-layered MoS_2 so as to utilize the lower bulk band gap[7] and higher electron (hole) mobilities, which are found to peak[42] at 470 (480) cm^2/Vs at approximately 50 nm MoS_2 thickness. As such, a band diagram for the HfO_2/MoS_2 (bulk) system has been *experimentally* determined and presented here.

Figure 5a shows an energy band diagram for the HfO_2/MoS_2 system developed from the experimentally determined valence band offset (VBO) and band gaps. After 100 cycles of HfO_2 ALD on MoS_2, XPS can provide a direct measurement of both the HfO_2 band gap and the VBO between MoS_2 and HfO_2.[43−48] Since the film is discontinuous, it is possible to obtain information about the 10 nm tall (~30 nm diameter) HfO_2 islands while using the MoS_2 core-levels as a reference to ensure that band bending does not affect the VBO measurement. Figure 5b shows the O 1s core-level spectra after 100 cycles of HfO_2 ALD. This energy loss feature is due to the onset of the interband transition between the valence band maximum and the conduction band minimum. After subtracting the contribution from the overlapping Hf 4s feature[48] (see Supporting Information), the separation between the O−Hf feature and the onset of the O 1s loss feature provides a measurement of the HfO_2 band gap to be 5.99 $\pm$ 0.33 eV. The photoconductivity of the MoS_2 provides a measure of the band gap of bulk MoS_2.[49] The photoconductivity onset energy is 1.23 $\pm$ 0.02 eV, as shown in Figure 5c. The VBO information can be obtained from the difference in the valence band maximum of the bare MoS_2 and HfO_2/MoS_2 (described in more detail in the Supporting Information). These spectra are shown in Figure 5d, where the VBO is measured as 2.67 $\pm$ 0.11 eV. The combination of these experimentally determined values is then shown graphically in the energy band diagram (Figure 5a), where the conduction band offset can be inferred to be 2.09 $\pm$ 0.35 eV.

CONCLUSION

In summary, we have investigated the ALD of HfO_2 on MoS_2 substrates and experimentally measured the band structure of the HfO_2/(bulk)MoS_2 system. XPS revealed no evidence of hafnium after half-cycle depositions, and it has been concluded that the weak adsorption of ALD precursors leads to their time-dependent desorption. Short purge times are found to result in the deposition of HfO_2 without any evidence of covalent bonding to the surface. Experimental evidence suggests that HfO_2 is more strongly adsorbed on the surface of MoS_2 than either of the individual precursors. Due to the relatively weak interactions of TDMA-Hf and H_2O with the MoS_2 surface, the direct deposition of HfO_2 by ALD using these precursors has been shown to lack scalability, and therefore, either surface functionalization approaches or alternative deposition methods will be necessary if scaled dielectrics on MoS_2 channels are to be realized. The disparity between prior reports of conformal thick ALD films on MoS_2 that had been exposed to combinations of organics and solvents and the results on nonconformal growth presented here can be attributed to the impact of organic and solvent residues on ALD nucleation that has also been presented here. The role of surface contaminants in the nucleation of ALD should not be overlooked, and the development of controlled functionalization will be required before MoS_2 transistors with high-quality high-κ/MoS_2 interfaces will be realized.

METHODS

MoS_2 (purchased from SPI supplies[51]) was cleaned by mechanical exfoliation using scotch tape. The samples were loaded into UHV within less than 10 min of exfoliation (or removal from the solvent in the case of the study presented in Figure 2). ALD was carried out in a PICOSUN ALD reactor attached to the

XPS/ISS analysis chamber by a UHV transfer module (<1 $\times$ 10^{-10} mbar), which allows for *in situ* characterization. The ALD process was modeled on that reported by Radisavljevic *et al.*,[6] and the full details are discussed in the Supporting Information. For the preparation of controllably contaminated samples, two samples were cleaned by mechanical exfoliation prior to PMMA spin-coating. For the spin-coating process, the samples were secured to a glass slide by taping the edges with Kapton tape. The PMMA was dissolved in chloroform and spin-coated at 3000 rpm for 1 min followed by 1000 rpm for 1 min. The PMMA was allowed to dry for 12 h in nitrogen. The securing Kapton tape was then removed from the MoS_2 edges. The samples were then placed into separate baths of acetone or NMP. After the spin-coating of these two samples, a further two samples were mechanically exfoliated and placed in separate baths of acetone or NMP. Just before the removal of all samples from their respective solvent baths, the final MoS_2 sample was cleaned by mechanical exfoliation. As such, all samples were either freshly cleaned or removed from a solvent bath within 10 min of loading into UHV. Since all samples were mounted on a single Ti plate, the subsequent ALD was then simultaneous on all samples.

Conflict of Interest: The authors declare no competing financial interest.

Acknowledgment. This work was supported in part by the Center for Low Energy Systems Technology (LEAST), one of six centers supported by the STARnet phase of the Focus Center Research Program (FCRP), a Semiconductor Research Corporation program sponsored by MARCO and DARPA. C.L.H., J.K., and C.B. acknowledge support from the Southwest Academy on Nanoelectronics sponsored by the Nanoelectronic Research Initiative and NIST. H.D. acknowledges support from the National Science Foundation (NSF) under ECCS Award No. 0925844.

Supporting Information Available: Additional information including further details of MoS_2 surface preparation, experimental process flow, atomic layer deposition conditions, characterization techniques, band gap and valence band offset measurements. Also included is a discussion of the lack of evidence for HfO_2–MoS_2 reactions and the possible adsorption mechanisms. This material is available free of charge *via* the Internet at http://pubs.acs.org.

REFERENCES AND NOTES

1. Novoselov, K.; Geim, A. K.; Morozov, S.; Jiang, D.; Zhang, Y.; Dubonos, S.; Grigorieva, I.; Firsov, A. Electric Field Effect in Atomically Thin Carbon Films. *Science* **2004**, *306*, 666–669.
2. Reina, A.; Jia, X.; Ho, J.; Nezich, D.; Son, H.; Bulovic, V.; Dresselhaus, M. S.; Kong, J. Large Area, Few-Layer Graphene Films on Arbitrary Substrates by Chemical Vapor Deposition. *Nano Lett.* **2008**, *9*, 30–35.
3. Li, X.; Cai, W.; An, J.; Kim, S.; Nah, J.; Yang, D.; Piner, R.; Velamakanni, A.; Jung, I.; Tutuc, E. Large-Area Synthesis of High-Quality and Uniform Graphene Films on Copper Foils. *Science* **2009**, *324*, 1312–1314.
4. Blake, P.; Brimicombe, P. D.; Nair, R. R.; Booth, T. J.; Jiang, D.; Schedin, F.; Ponomarenko, L. A.; Morozov, S. V.; Gleeson, H. F.; Hill, E. W. Graphene-Based Liquid Crystal Device. *Nano Lett.* **2008**, *8*, 1704–1708.
5. Banerjee, S. K.; Register, L. F.; Tutuc, E.; Reddy, D.; MacDonald, A. H. Bilayer Pseudospin Field-Effect Transistor (Bisfet): A Proposed New Logic Device. *IEEE Electron Device Lett.* **2009**, *30*, 158–160.
6. Radisavljevic, B.; Radenovic, A.; Brivio, J.; Giacometti, V.; Kis, A. Single-Layer MoS_2 Transistors. *Nat. Nanotechnol.* **2011**, *6*, 147–150.
7. Liu, H.; Ye, P. D. MoS_2 Dual-Gate Mosfet with Atomic-Layer-Deposited Al_2O_3 as Top-Gate Dielectric. *IEEE Electron Device Lett.* **2012**, *33*, 546–548.
8. Zhou, S.; Gweon, G.-H.; Fedorov, A.; First, P.; De Heer, W.; Lee, D.-H.; Guinea, F.; Neto, A. C.; Lanzara, A. Substrate-Induced Bandgap Opening in Epitaxial Graphene. *Nat. Mater.* **2007**, *6*, 770–775.
9. Wang, Q. H.; Kalantar-Zadeh, K.; Kis, A.; Coleman, J. N.; Strano, M. S. Electronics and Optoelectronics of Two-Dimensional Transition Metal Dichalcogenides. *Nat. Nanotechnol.* **2012**, *7*, 699–712.
10. Novoselov, K.; Jiang, D.; Schedin, F.; Booth, T.; Khotkevich, V.; Morozov, S.; Geim, A. Two-Dimensional Atomic Crystals. *Proc. Natl. Acad. Sci. U.S.A.* **2005**, *102*, 10451–10453.
11. Jena, D.; Konar, A. Enhancement of Carrier Mobility in Semiconductor Nanostructures by Dielectric Engineering. *Phys. Rev. Lett.* **2007**, *98*, 136805.
12. Jang, C.; Adam, S.; Chen, J.-H.; Williams, E.; Das Sarma, S.; Fuhrer, M. Tuning the Effective Fine Structure Constant in Graphene: Opposing Effects of Dielectric Screening on Short- and Long-Range Potential Scattering. *Phys. Rev. Lett.* **2008**, *101*, 146805.
13. Wang, H.; Yu, L.; Lee, Y.-H.; Shi, Y.; Hsu, A.; Chin, M. L.; Li, L.-J.; Dubey, M.; Kong, J.; Palacios, T. Integrated Circuits Based on Bilayer MoS_2 Transistors. *Nano Lett.* **2012**, *12*, 4674–4680.
14. Fang, H.; Chuang, S.; Chang, T. C.; Takei, K.; Takahashi, T.; Javey, A. High-Performance Single Layered WSe_2 p-FETs with Chemically Doped Contacts. *Nano Lett.* **2012**, *12*, 3788–3792.
15. Farmer, D. B.; Gordon, R. G. Atomic Layer Deposition on Suspended Single-Walled Carbon Nanotubes *via* Gas-Phase Noncovalent Functionalization. *Nano Lett.* **2006**, *6*, 699–703.
16. Kim, S.; Nah, J.; Jo, I.; Shahrjerdi, D.; Colombo, L.; Yao, Z.; Tutuc, E.; Banerjee, S. K. Realization of a High Mobility Dual-Gated Graphene Field-Effect Transistor with Al_2O_3 Dielectric. *Appl. Phys. Lett.* **2009**, *94*, 062107.
17. Alaboson, J. M. P.; Wang, Q. H.; Emery, J. D.; Lipson, A. L.; Bedzyk, M. J.; Elam, J. W.; Pellin, M. J.; Hersam, M. C. Seeding Atomic Layer Deposition of High-k Dielectrics on Epitaxial Graphene with Organic Self-Assembled Monolayers. *ACS Nano* **2011**, *5*, 5223–5232.
18. Lee, B.; Mordi, G.; Kim, M. J.; Chabal, Y. J.; Vogel, E. M.; Wallace, R. M.; Cho, K. J.; Colombo, L.; Kim, J. Characteristics of High-k Al_2O_3 Dielectric Using Ozone-Based Atomic Layer Deposition for Dual-Gated Graphene Devices. *Appl. Phys. Lett.* **2010**, *97*, 043107.
19. Liu, H.; Xu, K.; Zhang, X.; Ye, P. D. The Integration of High-k Dielectric on Two-Dimensional Crystals by Atomic Layer Deposition. *Appl. Phys. Lett.* **2012**, *100*, 152115.
20. Pirkle, A.; McDonnell, S.; Lee, B.; Kim, J.; Colombo, L.; Wallace, R. M. The Effect of Graphite Surface Condition on the Composition of Al_2O_3 by Atomic Layer Deposition. *Appl. Phys. Lett.* **2010**, *97*, 082901.
21. McDonnell, S.; Pirkle, A.; Kim, J.; Colombo, L.; Wallace, R. M. Trimethyl-Aluminum and Ozone Interactions with Graphite in Atomic Layer Deposition of Al_2O_3. *J. Appl. Phys.* **2012**, *112*, 104110.
22. Hausmann, D. M.; Kim, E.; Becker, J.; Gordon, R. G. Atomic Layer Deposition of Hafnium and Zirconium Oxides Using Metal Amide Precursors. *Chem. Mater.* **2002**, *14*, 4350–4358.
23. McDonnell, S.; Dong, H.; Hawkins, J. M.; Brennan, B.; Milojevic, M.; Aguirre-Tostado, F. S.; Zhernokletov, D. M.; Hinkle, C. L.; Kim, J.; Wallace, R. M. Interfacial Oxide Re-Growth in Thin Film Metal Oxide III–V Semiconductor Systems. *Appl. Phys. Lett.* **2012**, *100*, 141606.
24. Powell, C. J.; Jablonski, A. NIST Electron Effective Attenuation Length Database, *SRD 82. U.S. Department of Commerce*; NIST: Gaithersburg, MD, 2001.
25. Brongersma, H. H.; Draxler, M.; de Ridder, M.; Bauer, P. Surface Composition Analysis by Low-Energy Ion Scattering. *Surf. Sci. Rep.* **2007**, *62*, 63–109.
26. Liu, H.; Ye, P. D. MoS_2 Dual-Gate Mosfet with Atomic-Layer-Deposited Al_2O_3 as Top-Gate Dielectric. *arXiv:1112.4397* **2011**, DOI: 10.1109/LED.2012.218452.
27. Qiu, H.; Pan, L.; Yao, Z.; Li, J.; Shi, Y.; Wang, X. Electrical Characterization of Back-Gated Bi-layer MoS_2 Field-Effect Transistors and the Effect of Ambient on Their Performances. *Appl. Phys. Lett.* **2012**, *100*, 123104.

28. Pirkle, A.; Chan, J.; Venugopal, A.; Hinojos, D.; Magnuson, C. W.; McDonnell, S.; Colombo, L.; Vogel, E. M.; Ruoff, R. S.; Wallace, R. M. The Effect of Chemical Residues on the Physical and Electrical Properties of Chemical Vapor Deposited Graphene Transferred to SiO_2. *Appl. Phys. Lett.* **2011**, *99*, 122108.
29. Lin, Y.-C.; Lu, C.-C.; Yeh, C.-H.; Jin, C.; Suenaga, K.; Chiu, P.-W. Graphene Annealing: How Clean Can It Be? *Nano Lett.* **2012**, *12*, 414–419.
30. Lee, Y. H.; Zhang, X. Q.; Zhang, W. J.; Chang, M. T.; Lin, C. T.; Chang, K. D.; Yu, Y. C.; Wang, J. T. W.; Chang, C. S.; Li, L. J.; *et al.* Synthesis of Large-Area MoS_2 Atomic Layers with Chemical Vapor Deposition. *Adv. Mater.* **2012**, *24*, 2320–2325.
31. van der Zande, A. M.; Huang, P. Y.; Chenet, D. A.; Berkelbach, T. C.; You, Y. M.; Lee, G. H.; Heinz, T. F.; Reichman, D. R.; Muller, D. A.; Hone, J. C. Grains and Grain Boundaries in Highly Crystalline Monolayer Molybdenum Disulphide. *Nat. Mater.* **2013**, *12*, 554–561.
32. Bowker, M. The Role of Precursor States in Adsorption, Surface Reactions and Catalysis. *J. Phys.: Condens. Matter* **2010**, *22*, 263002.
33. Kim, S.; Konar, A.; Hwang, W. S.; Lee, J. H.; Lee, J.; Yang, J.; Jung, C.; Kim, H.; Yoo, J. B.; Choi, J. Y.; *et al.* High-Mobility and Low-Power Thin-Film Transistors Based on Multilayer MoS_2 Crystals. *Nat. Commun.* **2012**, *3*, 1011.
34. Bertolazzi, S.; Krasnozhon, D.; Kis, A. Nonvolatile Memory Cells Based on MoS_2/Graphene Heterostructures. *ACS Nano* **2013**, *7*, 3246–3252.
35. Salmani-Jelodar, M.; Tan, Y.; Klimeck, G. Single Layer MoS_2 Band Structure and Transport. In *2011 International Semiconductor Device Research Symposium* 2011; p 59.
36. Plechinger, G.; Schrettenbrunner, F. X.; Eroms, J.; Weiss, D.; Schuller, C.; Korn, T. Low-Temperature Photoluminescence of Oxide-Covered Single-Layer MoS_2. *Phys. Status Solidi R* **2012**, *6*, 126–128.
37. Yun, W. S.; Han, S. W.; Hong, S. C.; Kim, I. G.; Lee, J. D. Thickness and Strain Effects on Electronic Structures of Transition Metal Dichalcogenides: 2H-MX_2 Semiconductors (M = Mo, W; X = S, Se, Te). *Phys. Rev. B* **2012**, *85*, 033305.
38. Liang, Y.; Huang, S.; Soklaski, R.; Yang, L. Quasiparticle Energy and Band Offsets of Monolayer of Molybdenum and Tungsten Chalcogenides. *arXiv:1306.0620* **2013**, DOI: 10.1063/1.4816517.
39. Kang, J.; Tongay, S.; Zhou, J.; Li, J. B.; Wu, J. Q. Band Offsets and Heterostructures of Two-Dimensional Semiconductors. *Appl. Phys. Lett.* **2013**, 102.
40. Fuhrer, M. S.; Hone, J. Measurement of Mobility in Dual-Gated MoS_2 Transistors. *Nat. Nanotechnol.* **2013**, *8*, 146–147.
41. Radisavljevic, B.; Kis, A. Measurement of Mobility in Dual-Gated MoS_2 Transistors. *Nat. Nanotechnol.* **2013**, *8*, 147–148.
42. Bao, W. Z.; Cai, X. H.; Kim, D.; Sridhara, K.; Fuhrer, M. S. High Mobility Ambipolar Mos_2 Field-Effect Transistors: Substrate and Dielectric Effects. *Appl. Phys. Lett.* **2013**, *102*, 042104.
43. Bell, F.; Ley, L. Photoemission Study of SiO_x ($0 \leq x \leq 2$) Alloys. *Phys. Rev. B* **1988**, *37*, 8383.
44. Chambers, S. A.; Droubay, T.; Kaspar, T. C.; Gutowski, M. Experimental Determination of Valence Band Maxima for $SrTiO_3$, TiO_2, and SrO and the Associated Valence Band Offsets with Si(001). *J. Vac. Sci. Technol., B* **2004**, *22*, 2205–2215.
45. Miyazaki, S.; Nishimura, H.; Fukuda, M.; Ley, L.; Ristein, J. Structure and Electronic States of Ultrathin SiO_2 Thermally Grown on Si(100) and Si(111) Surfaces. *Appl. Surf. Sci.* **1997**, *113*, 585–589.
46. Vitchev, R.; Pireaux, J.; Conard, T.; Bender, H.; Wolstenholme, J.; Defranoux, C. X-ray Photoelectron Spectroscopy Characterisation of High-k Dielectric Al_2O_3 and HfO_2 Layers Deposited on SiO_2/Si Surface. *Appl. Surf. Sci.* **2004**, *235*, 21–25.
47. Hudait, M. K.; Zhu, Y. Energy Band Alignment of Atomic Layer Deposited HfO_2 Oxide Film on Epitaxial (100)Ge, (110)Ge, and (111)Ge Layers. *J. Appl. Phys.* **2013**, *113*, 114303.
48. Ohta, A.; Murakami, H.; Higashi, S.; Miyazaki, S. Determination of Energy Band Alignment in Ultrathin Hf-Based Oxide/Pt System. 15th International Conference on Thin Films; *J. Phys. Conf. Ser.* **2013**, *417*, 012012.
49. Afanas'ev, V. V. *Internal Photoemission Spectroscopy: Principles and Applications*; Elsevier: Amsterdam, 2010.
50. Chan, J.; Balakchiev, M.; Thron, A.; Chapman, R.; Riley, D.; Song, S.; Jain, A.; Blatchford, J.; Shaw, J.; van Benthem, K. PtSi Dominated Schottky Barrier Heights of Ni (Pt) Si Contacts Due to Pt Segregation. *Appl. Phys. Lett.* **2013**, *102*, 123507.
51. Spi Supplies. http://www.2spi.com/.